Engineering Structures 266 (2022) 114556

Contents lists available at ScienceDirect

Engineering Structures

journal homepage: www.elsevier.com/locate/engstruct

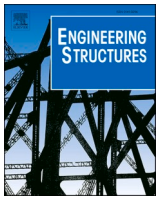

Brittle failure of laterally loaded self-tapping screw connections for cross-laminated timber structures

Boris Azinović [a], José Manuel Cabrero [b,*], Henrik Danielsson [c], Tomaž Pazlar [a]

[a] Slovenian National Building and Civil Engineering Institute (ZAG Ljubljana), Section for Timber Structures, Dimičeva ulica 12, Ljubljana, Slovenia
[b] University of Navarra, Wood Chair, Campus Universitario, 31009 Pamplona, Navarra, Spain
[c] Lund University, Faculty of Engineering LTH, Department of Construction Sciences, 221 00 Lund, Sweden

ARTICLE INFO

Keywords:
Cross-laminated timber
Connections
Brittle failure
Experimental testing
Analytical model
Overstrength

ABSTRACT

The performance of structural timber connections is of utmost importance since they control the global response of the building. A ductile failure mechanism on the global scale is desirable, especially in the design of structures in seismic areas, where dissipative components in which ductile failure modes need to be ensured are considered. Therefore, the knowledge of possible brittle failure modes of connections is crucial. The paper investigates the brittle failures of laterally loaded dowel-type connections in cross-laminated timber subjected to tensile load in a lap joint configuration through experimental investigations and analytical estimations. A set of 13 different test series has been performed with fully threaded self-tapping screws of 8 mm diameter and different lengths (40 to 100 mm) in cross-laminated timber composed of 3 or 5 layers (layer thickness range from 20 to 40 mm), giving rise to the activation of different brittle failure modes at different depths. Plug shear was among the most typically observed failure modes. A previously proposed model for the brittle capacity was applied to the tested connections at the characteristic level. As shown by the performed statistical analysis, the existing model is not reliable and mainly unconservative. A very low performance is observed (CCC = 0.299), but with a good correlation (c = 0.750) for the tests in the parallel direction. Further research work is required to improve the current model predictions and to gain a better understanding of the underlying resisting mechanisms.

1. Introduction

Nowadays, one of the best solutions for decarbonisation of the construction sector is to introduce more wood into building practices, which means that this material should not be used only for single-family housing, as was common practice in the 20th century. Consequently, there is a high demand for wood to be used in various types of structures, especially mid-rise (up to 10 storeys) and high-rise buildings (more than 10 storeys) that are the predominant type of buildings in dense urban environments. With the development of high-performance engineered wood products (EWPs) such as cross-laminated timber (CLT), building with wood has enabled larger and taller buildings to be erected. However, due to the relatively short period since emerging and implementation of advanced EWPs and their new structural systems have been present on the market, the knowledge and experience using these materials for high-rise buildings is still limited.

Particularly in the case of mid- and high-rise buildings, the performance of their structural connections is of utmost importance, since they control the global response of the building. However, the knowledge on the response of timber connections in CLT structures is still scarce and it mainly comes from the technical documents from commercial connection types, and proprietary connections, e.g. European Technical Assessment documents (ETAs), technical sheets and others. Few works describe a general approach to determine the characteristics of CLT connections such as the load-bearing capacity and stiffness, see e.g. [1,2].

For general safety reasons, the occurrence of a ductile failure mechanism on the global scale of the building is desirable. This is the case especially in the design of structures in seismic areas, where dissipative components in which ductile failure modes need to be ensured are considered. Therefore, the existence of inadvertent brittle failure modes of connections can be of utmost importance. For structural design, the concept and use of an overstrength factor [3] is introduced, which intends to increase the difference in load-bearing capacity

* Corresponding author.
E-mail addresses: boris.azinovic@zag.si (B. Azinović), jcabrero@unav.es (J.M. Cabrero), henrik.danielsson@construction.lth.se (H. Danielsson), tomaz.pazlar@zag.si (T. Pazlar).

https://doi.org/10.1016/j.engstruct.2022.114556
Received 13 December 2021; Received in revised form 27 May 2022; Accepted 13 June 2022
Available online 20 June 2022

between ductile and brittle failure mechanisms, so that a ductile failure is favoured.

Recent works have been done related to the risk of brittle failure of connections in timber structures. In previous reports, connections have been found to be one of the main issues related to failure or damage to timber constructions (e.g. [4,5]). Works were done in the COST Action FP1402 to review existing models and to revise the understanding of practitioners of such problems [6]. It was found that most of them were not aware of the importance of brittle failure of connections [7]. Most of the related work on brittle failure of connections has been done on glulam (GL) and laminated veneer lumber (LVL) members [8–11], while corresponding research work on CLT elements appears to be very limited. Zarnani and Quenneville proposed an analytical model as a derivation of a previously proposed model, accompanied by some verification tests of connections in CLT elements [12].

The paper deals with experimental investigations and analytical estimations of high-load bearing connections in CLT structures as a direct response to the problem of structural connections in high-rise buildings. The horizontal loads due to wind and earthquakes (in seismically active areas) increase with building size. Higher loads consequently demand better performing and efficient connections between the structural elements to transfer the loads to the foundations and to assure the overall structural resistance and stability. Therefore, there is a need for new high-performance structural connections for tall timber and hybrid structures. There is furthermore a need for a set of structural design guidelines regarding which types of connections are suitable for different structural concepts and loading scenarios, how to execute the connections as well as how to computationally evaluate their load-bearing capacity.

High performance (in terms of load-bearing capacity and stiffness) connections may reduce the overall safety of the structural system due to the introduction of possible brittle failure modes of the timber matrix which, in addition to a different structural response, reduce the predicted load capacity due to a premature unexpected failure. Therefore, it is required to increase the knowledge on such brittle responses in CLT connections, especially in the case of hold-down connections, which are subjected to a combination of tensile and shear loads. The paper investigates the brittle failure of dowel-type CLT connections with self-tapping screw fasteners subjected to tensile load, which may be regarded as the usual design condition for hold-down connections.

This paper is organized as follows: Section 2 presents some of the existing knowledge on the brittle failure of CLT connections; Section 3 presents the test campaign on CLT connections, while Section 4 elaborates the application of existing models to these tests.

2. Brittle failure of cross-laminated timber connections

The design of CLT connections is not yet considered within codes and standards normative in the European framework, as CLT is not yet covered as a product in the current Eurocode 5 [13]. The design of CLT connections is already considered in the American [14] and Canadian regulations [15]. Additionally, practitioners [16] make use of several handbooks [17–19] and the ETAs from the CLT and fastener producers (e.g. [20–22]).

The dominating existing design philosophy of connections aims at ensuring a load-bearing capacity related to a ductile failure mode, to be achieved by a combination of two ductile mechanisms: development of plastic hinges in the fasteners and embedment failure in the timber element. The load-bearing capacity of the connection is then reduced by considering a group effect, by the use of a so-called *effective number of fasteners*, which relates to load distribution among fasteners, stress concentrations and the possible occurrence of brittle failure modes of connections.

In the case of the Eurocode 5, the model for the effective number of fasteners considered mainly splitting failure [23]. In 2004, it was found necessary to include an informative annex to assess block shear failure in groups of fasteners, which remains in the current version [13]. In the future Eurocode 5, currently under preparation, a newly developed chapter will be dedicated to the brittle failure of connections.

In the case of Canada [15] and New Zealand [24,25], dedicated models for the evaluation of load-bearing capacity regarding brittle failure modes of solid wood connections are already included in the design standards. However, in the Canadian standard [15], brittle failure of connections in CLT elements is disregarded, by explaining that they are not expected due to the reinforcement induced by the cross-layers.

Possible brittle failure modes are *block shear*, *plug shear*, *row shear, step shear,* or *net tensile failure*. Several models for the brittle failure of connections have been developed for the different possible failure modes in solid timber connections [8,9]. They all define the load capacity for each of the failure planes, and then consider different combinations for the obtention of the resulting load-bearing capacity of the connection concerning brittle failure. However, due to the load distribution among adjacent layers within a CLT element, that is, the reinforcement obtained by the cross-layers, these models cannot be directly applied to CLT.

A typical connection in CLT structures consists of a 3D-steel plate (i.e. hold down or steel angle bracket), which is connected to the timber elements using small-diameter partially penetrating fasteners, such as screws, anchor nails, or rivets (Fig. 2). Hence, expected brittle failure modes relate to different modes of the failure commonly referred to as *plug shear* failure, which involves the associated failure onset of three different planes, related to different mechanisms: *head tensile, lateral shear*, and *bottom shear*, which are defined by the perimeter of the connection area.

The model from Zarnani and Quenneville [26], though originally developed for glulam and LVL, was expanded to consider connections in CLT [12]. This model considers six different failure modes for plug shear (see Fig. 1); partial failure of the outer layer (A), total failure of the outer layer (B), first layer and partial second (C), first and second (D), additional third layer partial (E), complete third layer (F). The different failure modes A-F are assumed to be related to the effective length of the fastener, that is, to the considered penetration of the fastener in the layers (obtained from a beam on elastic foundation model).

Additional failure modes (also shown in Fig. 1) may appear for these connections: *step shear*, in which the torn-out block corresponds to the whole width of the panel, and the *net tension* failure of the complete CLT cross-section.

The model is a stiffness-based model, in which the load-bearing capacity is obtained based on the force distribution obtained by considering the stiffness of the involved failure planes.

As main model assumptions, the contributions from the lateral planes are dismissed (as there is no control on the positioning of the unbounded interface of the parallel boards), and only the bottom and head planes are considered.

Two different bottom planes are considered (see Fig. 1): the adjacent shear planes (*a*) between the top parallel layer and cross layer below, and the bottom shear plane (*d*) in the cross-layer. The reinforcing effect of the cross-layers which contribute to transferring the load to the adjacent outer and inner parallel laminations is considered in the corresponding formulation of the bottom planes.

Different considerations on the stiffness of the failure planes, related to the assumed load distribution within adjacent layers, are used, depending on the fastener penetration depth. Not all the previously described planes are always considered: mode A involves only *bottom* and *head* planes, while mode F, only *head* and *adjacent* ones.

After obtaining an initial failure mode, the model needs to be recalculated again, dismissing the already failed plane, to verify whether the residual planes may resist a higher load. Moreover, in the case of failure modes involving the second cross-layer, after the failure of the head plane, the resulting capacity cannot be greater than that obtained from considering a failure mechanism of the torn-out timber block as a

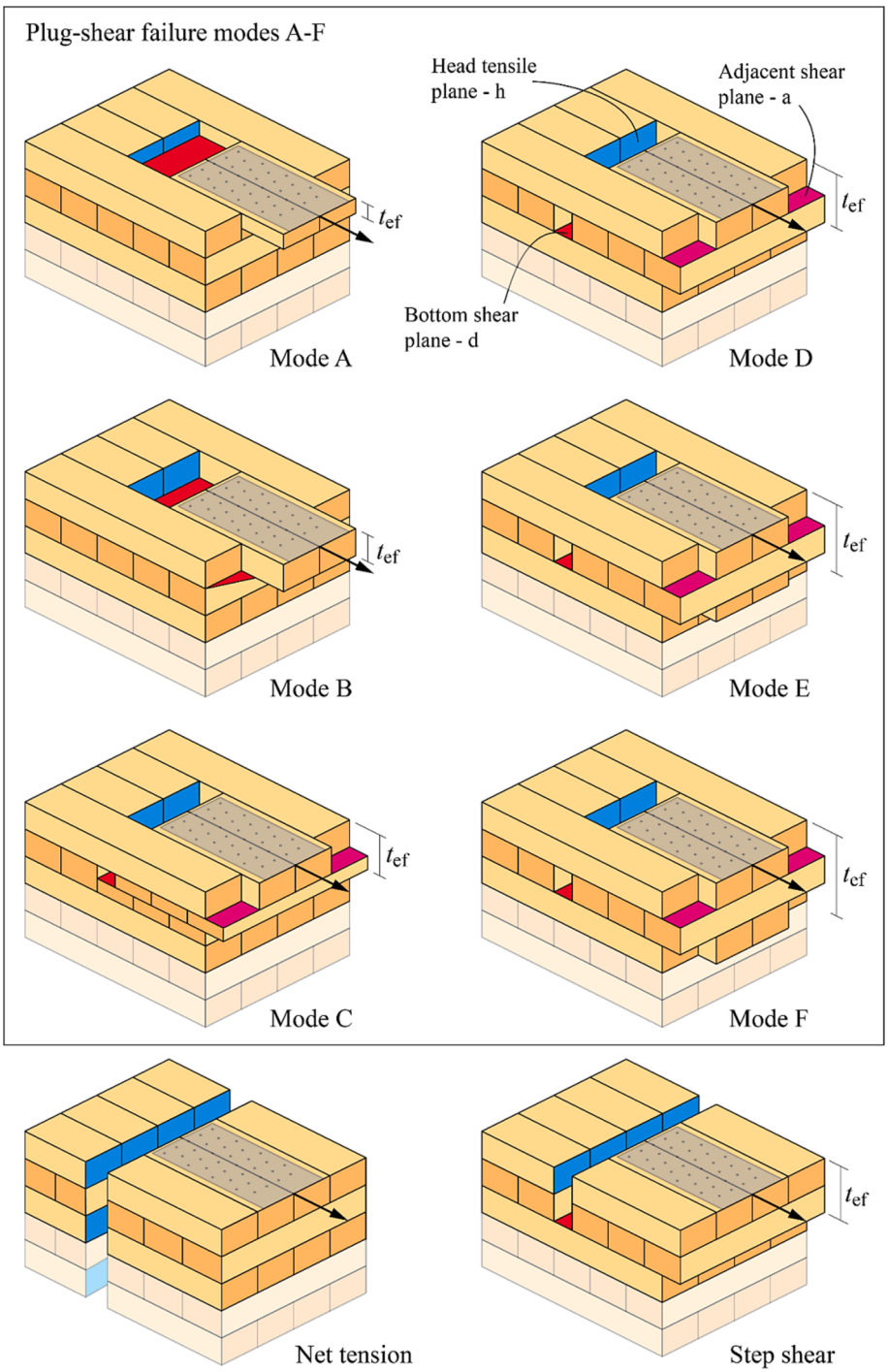

Fig. 1. Different possible failure modes of plug-shear failure of CLT connections (modified after [12]).

virtual connection to the plate, calculated from the yielding capacity of the fastener and the rolling shear resistance of the bottom plane (this mechanism is called herein as yielding-rolling). The reader is referred to [12] for a more detailed description of the model, including the applicable equations.

Comparison between experimental findings, regarding load-bearing capacities and failures modes, and predictions according to the model are presented in Section 4.

3. Tests campaign and results

3.1. Materials

The tests presented in the paper have been performed in the Laboratory for Structures of the Slovenian National Building and Civil Engineering Institute. To study brittle failure modes of dowel-type CLT connections, a set of 13 different test series has been tested, see Table 1. Four different types of CLT were used. Two of them were narrow-edge-bonded [21]: 3-layered (layup 30–40–30 mm) and 5-layered (layup 40–20–20–20–40 mm). The two remaining types of CLT were unbonded on the narrow edge [22]: 5-layered (layup 20–20–20–20–20 mm and

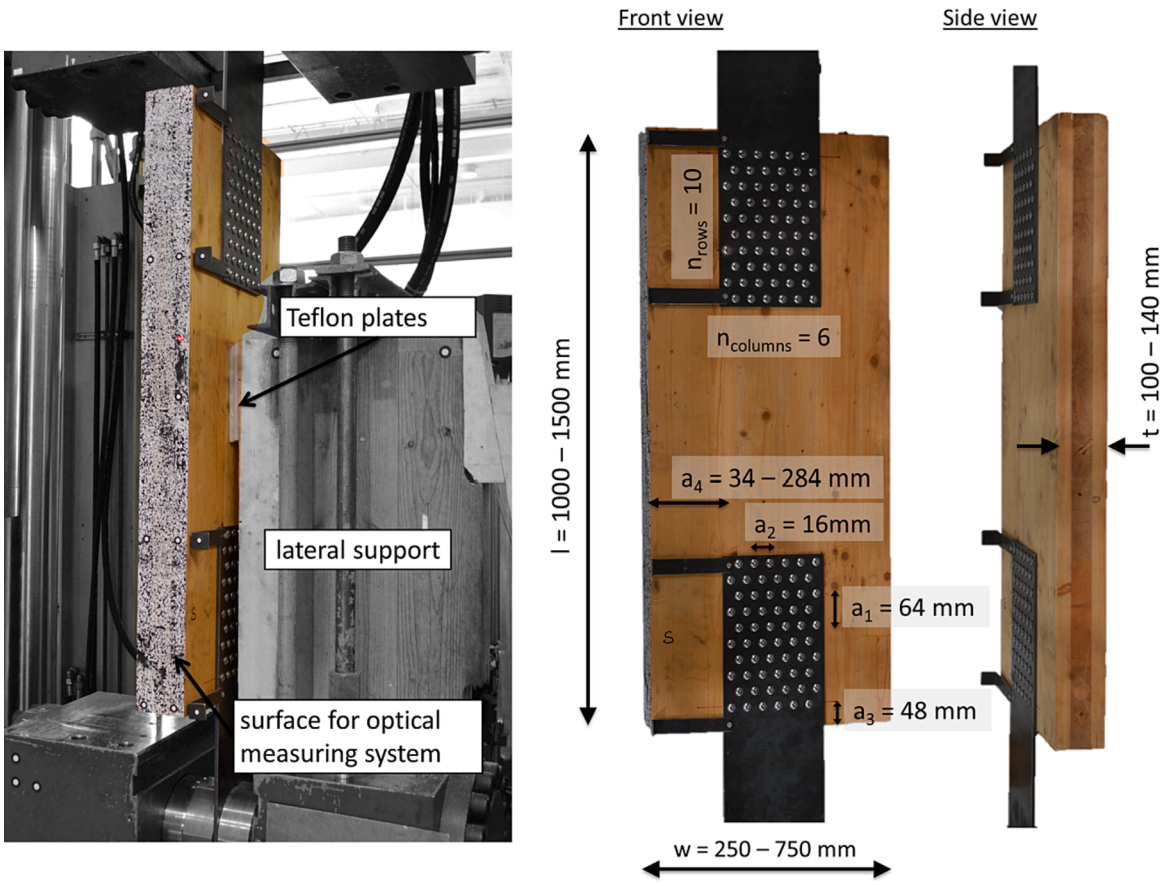

Fig. 2. Test set-up and test specimen with denotations.

Table 1
Basic characteristics of the specimens used in the experiments.

Test series	Number of tests	w [mm]	t [mm]	l [mm]	a_4 [mm]	CLT layers [mm]	α [°]	l_s [mm]	Lateral support	Moisture content [%]	Density [kg/m^3]
AB1	6	245	142	1228	34	40–20–20–20–40	0	40	no	14.6	469.2
AB2	6	250	142	1498	37	33–20–33–20–33	0	40	no	14.6	442.1
CD1	7	250	101	988	37	20–20–20–20–20	0	40	yes	12.9	445.8
CD2	7	251	101	1201	37	30–40–30	0	60	yes	15.0	468.1
CD2_90	6	248	101	1200	37	30–40–30	90	60	yes	14.2	481.4
CD3	6	500	101	1199	162	30–40–30	0	60	yes	13.3	470.9
CD3_90	3	500	101	1200	162	30–40–30	90	60	yes	13.3	460.6
CD4	6	743	101	1198	283	30–40–30	0	60	yes	14.0	472.7
CD5	6	250	140	1200	35	33–20–33–20–33	0	60	yes	15.0	429.8
CD5_90	8	250	140	1200	35	33–20–33–20–33	90	60	yes	14.7	438.5
EF1	4	250	100	1000	35	20–20–20–20–20	0	100	yes	13.0	454.6
EF2	6	250	140	1200	35	33–20–33–20–33	0	100	yes	15.8	414.8
EF3	3	500	140	1200	165	33–20–33–20–33	0	100	yes	12.3	434.4

Notations: w = CLT width (average value for all specimens), t = CLT thickness (average value for all specimens), l = CLT length (average value for all specimens), a_4 = edge distance of the screws (average value for all specimens), α = angle between the tensile load and grain of the boards in the outer layer and l_s = screw length (nominal value).

33–20–33–20–33 mm). According to the technical specifications supplied by the producers, all four types of CLT were manufactured from softwood (European spruce or similar) timber boards of strength class C24 and glued together with one-component polyurethane adhesive.

Fasteners used in the study were carbon steel fully threaded self-tapping screws with a diameter of 8 mm and a characteristic yield moment $M_{y,k}$ = 20 Nm (declared by the producer in its technical information) [20]. Three different screw lengths were used (40, 60 and 100 mm).

The steel plates were of dimensions 208 × 800 × 8 mm and a steel grade S355 (characteristic yield strength $f_{y,k}$ = 355 MPa). The hole pattern was the same for all test configurations and was designed according to the provisions of Eurocode 5 [13] (Fig. 2).

3.2. Specimens

Dowel type connections are usually designed to achieve a ductile failure mode by yielding of the dowels or the connecting steel plate. However, for this study, the connections were designed such that dowel yielding should be limited to be able to analyse the possible brittle

failure modes. This approach was adopted to determine the weak points and the upper load-bearing capacity for the considered dowel-type connections. The findings from Zarnani and Quenneville [12] were used to design the test specimens.

Steel plates were connected by 60 screws to the CLT elements at the top and bottom sides according to the basic configuration depicted in Fig. 2, where also the spacing of screws is shown; $a_1 = 64$ mm, $a_2 = 16$ mm, $a_3 = 48$ mm and $a_4 = 34$–283 mm (depending on the CLT width). The specimens varied in terms of their width (w), CLT layup, orientation of the boards in the outer layer measured in relation to the tensile load (α) and screw length (l_s). Basic characteristics of the specimens are shown in Table 1, where the dimensions w, t, l and a_4 are given as average values of all specimens within the respective test series. Moisture content was determined by electrical resistance method using a handheld (EN 13183–1:2002/AC:2003) metre on three locations for each specimen, and mean values for all test configurations are provided in Table 1 accordingly. Similarly, a mean value of density (based on the measured self-weight) is given for each configuration separately. Three to eight specimens were tested for each test configuration, and altogether 74 tests were performed.

For the selected *pull-pull* test configuration, in some cases (especially for CLT with thickness 100 mm) the specimens deformed also in the lateral direction at the middle of the specimen (up to 3 mm lateral displacement at high tensile load). To avoid the influence of load eccentricity, a lateral support with a Teflon sliding bearing was used for all specimens, except for series AB1 and AB2 (CLT thickness 140 mm), where the influence of load eccentricity did not prove to be significant. The presence of lateral support is indicated for each test series in Table 1.

3.3. Test set-up and protocol

The connections were investigated using a *pull-pull* test configuration

series AB2; combination of row shear and plug shear, mode A

series CD3_90; step shear and plug shear, mode C

series EF3; predominantly plug shear, mode E

series EF1; tensile failure of the CLT cross section

series CD2_90; step-shear failure

Fig. 3. Examples of failed specimens.

(Fig. 2) with nominally equal connections on both sides of the specimen. The monotonic tension tests were performed using a Universal testing machine Zwick Z2500Y under displacement control. The tests were conducted following the standard ISO 6891:1983 [27]. The displacements in each test were measured on the narrow surface of the specimen and additionally at 14 discrete points using a digital image correlation (DIC) system. All tests were recorded at a 5 Hz acquisition rate utilising two 12MPx CCD cameras. The relative displacement of each connection was determined as the difference between the displacement of the steel plate and the displacement at the middle of the CLT specimen.

4. Results

The performed experiments exposed several different failure modes, which were further documented and analysed to assess the performance of the currently existing model [12]. The possible failure modes were identified descriptively, distinguishing between the following: *row shear*, *plug shear*, *step shear, and net tension* (tensile failure of the CLT gross cross-section), or their combinations. Additionally, capital letters (A-F) are used to indicate where the failure occurred as described in [19] and shown in Figs. 1 and 3. The failure modes were predicted prior to the experiments based on the length of the screws and the test series were named accordingly: series AB (mode A and B), series CD (mode C and D), series EF (mode E and F), where the possibility of complete tensile failure was not included in the naming.

As expected, all of the tested specimens failed in a brittle manner, but not always in plug-shear, which was the only mode given in the previous work [12]. Although plug shear was the most representative failure mode, this failure mode occurred in combination with row shear for some specimens (Fig. 3). In series EF1 a net tensile failure of the CLT cross-section (Fig. 3) occurred. For specimens with perpendicular to the grain orientation ($\alpha = 90°$), step shear was reached (series CD2_90, CD3_90 and CD5_90).

In Fig. 4 all load–displacement curves are shown, where the response is given jointly for both connections (on each side of the specimen) in a single curve. The load–displacement curves indicate that in most cases a sudden drop of the load was obtained after reaching the load-bearing capacity. This proves that the response of connections is brittle, although in some test series plastic deformation of the screws occurred prior to failure. In the elastic state, the two connections of each specimen reach approximately the same relative displacement at equal force. Nevertheless, for the calculation of stiffness, a mean value of stiffness was determined for each specimen from the two connections on each side (Table 2).

In most of the tests, and as shown by the resulting ductility indexes, brittle failure happened after yielding of the fasteners began, so it should be considered that brittle failure occurred in the mixed range, with ongoing yielding of the fastener.

In some test series, two different failure modes were observed, either row shear or plug shear failure. Specimens with row shear failure experienced a higher ductility than specimens with plug shear, which may be observed in the load–displacement curves as a non-linear part of the curve (Fig. 4). As brittle failure relates to the failure of the timber matrix, dispersion of the results is expected and may be observed.

Table 2 summarises the results of the performed tests: mean ultimate load value F_T, stiffness $k_{10\text{-}40}$ – obtained according to EN 26891 [27] as secant stiffness between 10% and 40% of the ultimate load F_t, ductility index D_f – as defined in EN 12512 [28], the corresponding COV between the specimens in each configuration, and the most common failure modes achieved on each configuration are provided. For some test series, all specimens failed in the same manner while two or more failure modes were observed within other test series.

In those series where a comparable test series with loading in the perpendicular direction was performed (e.g. CD2, $\alpha = 0°$; and CD2_90, $\alpha = 90°$), the difference is noticeable already by comparing the load–displacement diagrams. In general, the perpendicular to the grain specimens ($\alpha = 90°$) reached much lower load-bearing capacities (cca. 35–40%) than the comparable specimens with $\alpha = 90°$. Similarly, also the stiffness values of the 90° specimens were much lower than for the 0° specimens (cca. 50% lower).

Since two nominally equal connections were tested simultaneously for each specimen, while only one of them failed, a probabilistic model was used to obtain the mean values ($F_{t,mean}$) and CoV for the ultimate load-bearing capacity values, considering the response of both simultaneously tested connections, but where just one of them fails. Hence, each test has been considered as a series system composed of two Weibull components (the two connections) with a common exponent c (since the two connections are nominally equal), where one of them has failed. The system capacity may then be expressed as.

$$R(x) = exp\left(- \left(\frac{x}{a_{sys}} \right)^{c} \right), \tag{01}$$

where a_{sys} is the parameter for the system of two connections, defined by $a_{sys} = \frac{a}{2^{\frac{1}{c}}}$, and a is the parameter for a single connection [29].

The characteristic load-bearing capacity values ($F_{t,char}$) were calculated according to the recommendations in the EN 14358:2016 [30]. Due to the low coefficient of variation (Table 2) for the mean values of the load-bearing capacity (CoV < 15%, except for CD3_90), the calculation for the characteristic values was simplified, and a normal distribution was assumed:

$$F_k = F_t - k_s(n)s_y \tag{02}$$

where F_t is the mean value (Table 2), k_s statistical factor for determining the 5% quantile for the one-sided 75% confidence level, n number of specimens (twice the number of tests), and s_y the standard deviation. It should be considered that, especially for those test series with a rather small number of test samples (e.g. CD3_90, EF1, EF_3) the precision and significance of the calculated characteristic values is rather limited.

From the results presented in Fig. 4 and Table 2, several important conclusions can be drawn:

- The increase of the specimens' width substantially increased the load-bearing capacity, while the elastic stiffness did not change significantly (Fig. 5). The increase of the width from 250 mm (series CD2) to 750 mm (series CD4) caused an approximate 45% increase in the load-bearing capacity, whereas the elastic stiffness increased by only 8%. A similar trend is noticeable also when comparing series EF2 to EF3, where the width of the specimen changed from 250 mm to 500 mm.
- A significant direct relationship may be found between the screw penetration length and the resulting connection stiffness. A stiffness increase of 70% is noticed between comparable series CD1 and EF1 (40 mm and 100 mm screw length), and series AB2 and CD5 (40 mm and 60 mm screw length), respectively. However, when comparing CD5 and EF2 (60 mm and 100 mm screw length) very similar results in terms of stiffness are obtained.
- However, a less significant increase in the load-bearing capacity is observed when these comparable series with different screw lengths (CD1 and EF1; AB2 and EF2) are considered, being just around 15%. The failure mechanisms of AB2 and EF2 series were similar, being the difference in the position of the bottom failed plane. In the case of test series AB2 and CD5 (same CLT type, but CD5 had screws of 60 mm length instead of 40 mm as in the series AB2) there was no significant increase, in both of which just one parallel layer is activated. In Fig. 5 the difference between the load-bearing capacity of short screw specimens (AB2) and long screw specimens (EF2) with comparable CLT is presented.
- As seen also from the load–displacement diagrams (Fig. 4), the different orientations of the outer layer substantially influenced both the stiffness and the load-bearing capacity. This can be seen by direct

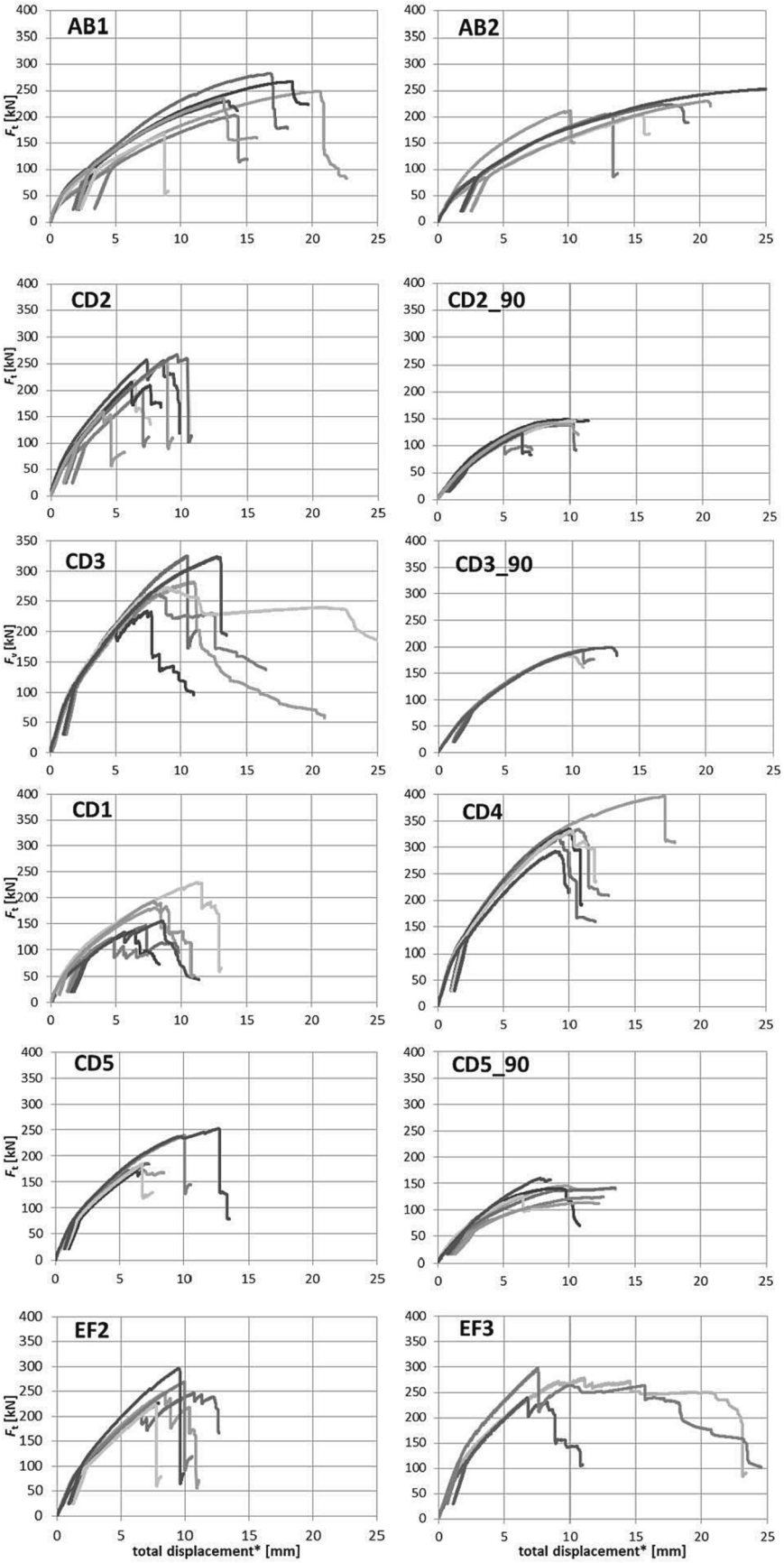

Fig. 4. Load-displacement diagrams of the performed tests for all test series. *Note: total displacement refers to a relative displacement of both connections, measured between both steel plates.

Table 2
Results obtained for all test series.

Test series	$F_{t,mean}$ [kN]	CoV [%]	$F_{t,char}$ [kN]	$k_{10\text{-}40}$ [kN/mm]	CoV [%]	$k_{40\text{-}90}$ [kN/mm]	CoV [%]	D_f [-]	CoV [%]	Failure mode
AB1	260.8	8.9	200.7	64.7	17.3	23.8	11.5	1.47	10.0	Mode A, Row/Plug
AB2	236.7	8.8	181.5	66.7	27.5	25.3	25.2	1.37	29.0	Mode A & B, Row/Plug
CD1	190.2	4.4	103.7	96.4	12.1	33.7	23.6	1.49	12.8	Mode C & D, Plug
CD2	246.7	6.7	173.5	124.1	24.4	49.9	13.9	1.51	15.0	Mode C, Plug
CD2_90	143.3	11.2	117.0	66.1	11.7	28.6	18.6	1.47	8.8	Mode C, Plug
CD3	304.6	8.3	229.6	146.1	12.4	47.3	9.0	1.47	6.1	Mode C, Row/Plug
CD3_90	196.8	29.0	181.0	77.8	8.9	31.9	5.0	1.49	3.5	Mode C, Plug
CD4	358.1	8.8	274.3	134.3	15.8	50.6	15.9	1.52	5.8	Mode C & D, Row/Plug
CD5	224.2	5.7	143.1	112.3	8.3	40.8	11.0	1.53	4.9	Mode C & D, Row/Plug
CD5_90	145.5	8.8	112.5	66.7	13.2	26.9	22.2	1.43	5.7	Mode C, Plug
EF1	224.9	4.9	124.2	166.2	20.6	53.9	11.5	1.41	13.5	Tensile specimen failure
EF2	269.1	8.6	205.1	110.5	7.0	43.7	16.6	1.61	19.7	Mode E, Row/Plug
EF3	286.7	11.7	229.7	173.5	27.7	51.5	12.7	2.26	44.1	Mode E, Row/Plug

Notations: $F_{t,mean}$ = mean ultimate load, $F_{t,char}$ = characteristic ultimate load, $k_{10\text{-}40}$ = secant stiffness between 10% and 40% F_t (elastic stiffness), $k_{40\text{-}90}$ = secant stiffness between 40% and 90% F_t and D_f = ductility index.

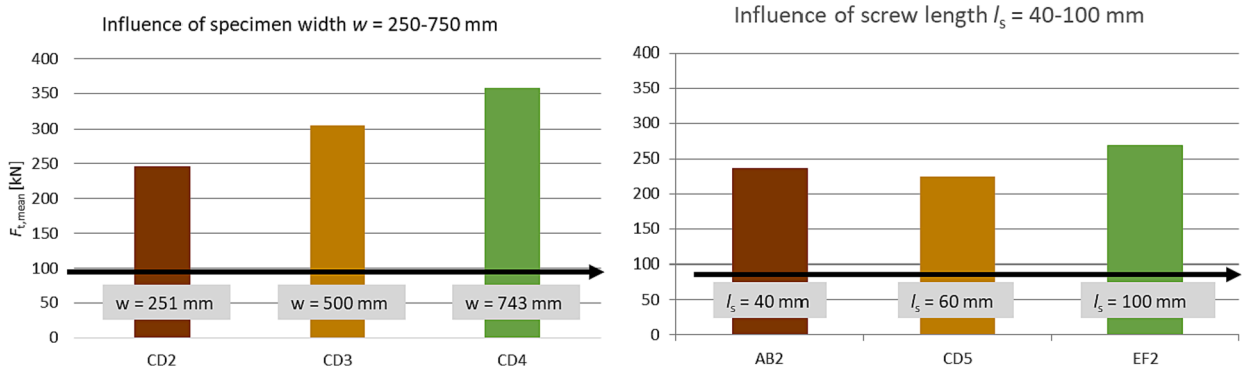

Fig. 5. Comparisons between (mean) load bearing capacities as a function of specimen width (left) and screw length (right).

comparison of the series CD2 to CD2_90, CD3 to CD3_90 and CD5 to CD5_90. The decrease of secant stiffness is approximately the same for all test series. The stiffness $k_{40\text{-}90}$ was reduced by 60–70% in comparison to the elastic stiffness $k_{10\text{-}40}$.

- The average ductility D_f of the specimens was around 1.5, except for the series EF3, where the obtained ductility is higher. However, this test series consisted only of three nominally equal tests and showed a large CoV.
- The influence of the different CLT layups on the connection response was not straightforward to interpret. From the tested specimens, it can be concluded that the elastic stiffness does not notably change when different CLT layups are used for the same connection (in terms of screw placement and screw length); less than 3% difference was found between series AB1 and AB2 and less than 10% difference between CD2 and CD5. On the other hand, the different CLT layups influenced the load-bearing capacity, depending on the penetration length of the screws with respect to the individual layers. The load-bearing capacity of series AB2 is reduced in comparison to AB1 since the failure mode changed – the specimens failed also along the glued surface between the first and the second layer (in addition to mode A, also mode B failures occurred). The same trend of load-bearing capacity reduction was obtained in the case of series CD5 in relation to CD2.
- The influence of CLT with edge-glued laminations compared to CLT with non-edge glued laminations is difficult to obtain from the performed experiments, since there are no directly comparable test series. To some extent, series AB1 and AB2 could be compared, however, the two CLT layups are quite different. The higher capacity for AB1 could indicate that specimens with glued edges may reach higher capacity due to the glued narrow edges of the laminations and not only due to the difference in the CLT layout.

4.1. Model assessment

As explained above, most of the existing models for assessment of the brittle failure of connections are not appropriate for CLT connections, mainly due to the reinforcing effect produced by the cross-layers. The model from Zarnani and Quenneville [27] was adapted to CLT [19], and it is the one used in this section for the assessment of the performed tests.

The values for timber strength and stiffness properties used as input for the models, shown in Table 3, were chosen from those declared by the producers in their technical specifications [21,22], corresponding to the given CLT with C24 outer layer (according to EN 338:2016 [31]; coniferous-softwood species, i.e. Picea abies; with a characteristic bending strength of 24 MPa).

The current model for ductile failure (European Yield Model, EYM), was applied as well, based on the proposals given by practice literature [2,17–19]. It must be clarified that the required embedment strength values are obtained from the declared characteristic density of the timber strength class [31], and assumed to be the same irrespective of the angle between force and fibre direction (that is, no influence of the layer orientation is considered). As a consequence, connections perpendicular to grain are predicted with the same ductile capacity as those parallel connections comparable to them.

Table 4 and Fig. 6 show the comparison of the model predictions against the characteristic experimental results. Additionally, values obtained by means of the European Yield Model are plotted, not including (fastener yielding onset) and including the rope effect

Table 3
Properties of the timber products used in this work, based on producer declared values [21,22].

Lamination strength class	ρ_m [kg/m^3]	$E_{0,m}$ [MPa]	G_m [MPa]	$G_{m,r}$ [MPa]	$f_{t,0,k}$ [MPa]	$f_{t,90,k}$ [MPa]	$f_{v,k}$ [MPa]	$f_{v,r,k}$ [MPa]
C24	380	12,000	690	50	14	0.12	4	1.8

Notations: ρ_m = mean density, $E_{0,m}$ = mean modulus of elasticity, G_m = mean shear modulus, $G_{m,r}$ = mean rolling shear modulus, $f_{t,0,k}$ = characteristic tension parallel to the grain strength, $f_{t,90,k}$= characteristic tension perpendicular to the grain strength, $f_{v,k}$= characteristic shear strength, and $f_{v,r,k}$ = characteristic rolling shear strength.

Table 4
Comparison of predicted capacities at the characteristic level: experimental results ($F_{T,char}$), results of the brittle model ($F_{br,pred}$), and ductile EYM capacity, considering ($F_{EYM+Rope}$) and not considering (F_{EYM}) the rope effect. Modes correspond to those shown in Fig. 1. Failed plane: d (bottom plane), h (head plane), a (adjacent plane), yr (yielding-rolling limit).

Test series	Test capacity $F_{T,char}$ [kN]	Brittle model $F_{br,pred}$ [kN]	Mode	Failed plane	Effective thickness t_{eff} [mm]	EYM without rope ef. F_{EYM} [kN]	EYM with rope ef. $F_{EYM+Rope}$ [kN]
AB1	200.7	223.1	A	*d*	30.2	121.3	176.1
AB2	181.5	226.8	A	*d*	30.2	121.3	176.1
CD1	103.7	176.4	C	*d*	30.2	121.3	176.1
CD2	173.5	250.9	C	*yr*	44.8	150.0	235.9
CD3	229.6	250.9	C	*yr*	44.8	150.0	235.9
CD4	274.3	247.3	C	*d*	44.8	150.0	235.9
CD5	143.1	207.2	C	*d*	44.8	150.0	235.9
EF1	124.2	215.7	E	*yr*	44.8	186.9	330.6
EF2	205.1	270.9	E	*yr*	64.0	186.9	330.6
EF3	229.7	270.9	E	*yr*	64.0	186.9	330.6
CD2_90	117.0	250.9	C	*yr*	44.8	150.0	235.9
CD3_90	181.0	250.9	C	*yr*	44.8	150.0	235.9
CD5_90	112.5	179.5	C	*d*	44.8	150.0	235.9

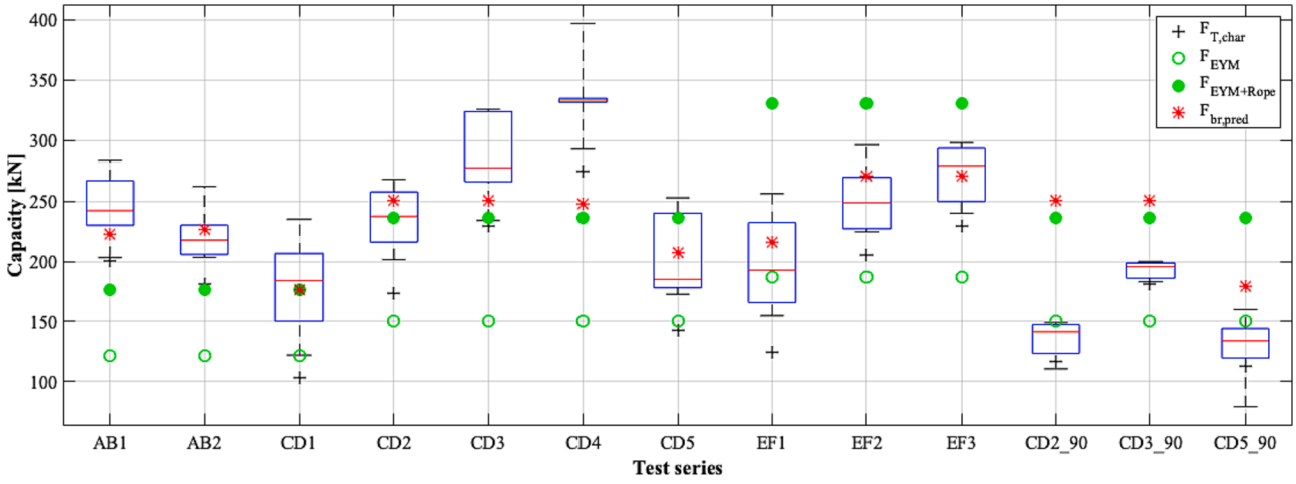

Fig. 6. Comparison of the model predictions and the experimental results of the tested connections.

(produced only at large displacements of the connection).

A statistical analysis considering different metrics was performed, whose results are given in Table 5. The used metrics allow for a comprehensive analysis of the response of the model, from overall performance by means of the coefficient of determination Q^2 [32,33] (reliable threshold value 0.70 [34], and best values closest to 1) and the Concordance Correlation Coefficient *CCC* [33–35] (again, values close to 1 are the best ones, with a recommended threshold value of 0.85). The *CCC* is used as an alternative metric to the Q^2, whose reliability has been questioned in the past [36,37]. Additionally, the mean relative error *MRE* (values around 10% are agreed as adequate), and its associated standard deviation *SD* are observed. The ability to provide a good correlation (independent of the quantitative prediction) is assessed by means of the rank correlation coefficient *c* [37] (values closer to 1 are the best), and the slope *m* of the linear fitting passing through the origin. The reader is referred to [10] for a more detailed description and discussion of the used metrics.

Table 5
Metrics for the model. Characteristic level.

	Q^2	*MRE*	*SD*	*m*	*c*	*CCC*
All tests	−0.838	0.351	0.183	1.255	0.597	0.299
Parallel dir.	−0.352	0.283	0.133	1.200	0.750	0.394
Perp. Dir.	−8.511	0.659	0.306	1.601	0.000	0.092

4.2. Parallel direction

A simple inspection of both Table 4 and Fig. 6 shows how the predicted ductile EYM capacity without the rope effect (fastener yielding

onset) is usually lower than the characteristic observed capacity for the connection (whose failure mode was actually brittle). As discussed above, most of the test series featured some ductility. When the rope effect is considered, the obtained EYM capacity for test series AB and CD is lower than the maximum experimental values, while it is higher than the experimental range in the case of the EF series.

In the case of the brittle model (which was developed for tests loaded in the parallel direction), it may be seen in Fig. 6 how the obtained values fall within the experimental values. However, they clearly surpass the experimental characteristic values up to 1.74 (EF1) and 2.14 (CD2_90). Only in the case of CD4 the model gets a conservative value, close to the characteristic one. However, being this the test in the series with the highest width, the model predicts a very similar capacity to those with a reduced width. It may be inferred that the current model does not capture the width influence on the load-bearing capacity.

All the predicted failure modes correspond to those in which failure happened at intermediate positions of the layers (modes A, C, or E), as observed in the tests. However, the model only accounts for plug shear, so the additionally observed row shear is not considered.

The failure mechanism corresponds either to the bottom plane (AB1, AB2, CD1, CD4 and CD5) or the yielding-rolling limit of the head tensile plane. There are no failures due to the adjacent plane.

Metrics in Table 5 confirm the general prediction ability of the model as quite poor. The overall performance (measured by Q^2 and *CCC*) is much lower than the recommended thresholds, with even a negative value for Q^2 (proof of a very deficient determination and high scatter). The obtained slope of the fitting line shows how the model tends to overestimate the brittle capacity. However, it features a good ability to capture the general relative trend, as shows the relatively good 0.750 value of the *c* correlation rank coefficient.

5. Perpendicular direction

There were three test series with $\alpha = 90^\circ$ (perpendicular to grain specimens) for Mode C (penetration in the second layer). Though the original model [12] is not applicable for such connections, a preliminary approach was done by modifying some parameters of the proposed equations for Mode C. The head tensile area was reduced to consider only the length of the fastener penetrating in the layer with laminations oriented parallel to the load, and the longitudinal shear strength, instead of the rolling shear strength, was considered for the bottom failure mechanism.

Based on these modifications, the same trend as in the comparable parallel connections was observed. The failure was controlled by the yielding-rolling limit for CD2_90 and CD3_90, and by the bottom plane for CD5_90. Again, the predicted brittle capacity is higher than the experimental one. More importantly, the modified model shows neither a good correlation, nor a good prediction ability. All the metrics are worse than those obtained for the tests in the parallel direction. Unconservative results may be due to the fact that the model originally was not intended for this layer orientation and, therefore, even with the assumed modifications, some additional modifications should be made in the future. Moreover, the model does not include the observed step shear failure.

Though not in the focus of this paper, the EYM values should be additionally discussed. The three tested connections have the same ductile capacity as the comparable parallel connections, since current practice literature [2,17,18] recommends using the same embedment strength regardless of the actual grain orientation. However, this leads to an overestimation of the ductile capacity as well.

6. Conclusions

The paper analyses the possibility of brittle failure modes for tensile loaded CLT with laterally-loaded screw connections, considering loading orientations both parallel and perpendicular to the direction of the laminations in the outer CLT layer. High-load bearing connections in CLT structures as analysed in this work would mainly be needed for hold-downs, where in most cases the connection is oriented parallel to the grain of the outer layer ($\alpha = 0^\circ$), and mainly designed for tensile loads.

The experimental results suggest that the load-bearing capacity of the connection increases with the width of the CLT specimen; e.g. a 45% increase was found between series CD2 ($w = 250$ mm) and series CD4 ($w = 750$ mm). However, increasing specimen width does not appear to affect the resulting elastic stiffness. The length of the screws was found to have a large impact on the elastic stiffness; e.g. an increase of more than 70% was found between 40 mm (series CD1) and 100 mm (series EF1) fastener lengths. The CLT layup does not seem to influence the elastic stiffness notably, while it influences the resulting load-bearing capacity, mainly concerning the penetration of the fastener into the different layers.

Though brittle failure mainly happens after the fasteners have started to yield, the ductility values are extremely low, around 1.5. Such connections with failure occurring in CLT, therefore, expose reduced capacity and ductility and are not appropriate for the design of structures in seismic areas, where much higher local ductility is required in connections.

Though typically the outer layer is oriented parallel to the load, in the case of CLT deep beams, CLT cantilevers, vertical connections between CLT walls or special architectural demands, also the perpendicular to the grain orientation of the outer layer ($\alpha = 90^\circ$) is possible. The results of the study, therefore, expose that it is crucial to recognize the even lower load-bearing capacities (around 60% for the brittle failure modes) in case of perpendicular to the grain orientation of the outer layer.

The analytical model for brittle failure of CLT connections found in the literature [19] and used in this study mainly obtains unconservative results. Its prediction ability is quite low, with most of the analysed metrics much lower than the recommended thresholds. Only the correlation ability in the case of the parallel direction connections shows a good performance. A modified model was developed for its application on perpendicular connections, with even worse results.

Moreover, the existing proposal, based on a stiffness model, is quite complex and cumbersome to apply. Future proposals should be developed aiming not only at an improved prediction ability but also at a simpler formulation.

Additionally, it has been shown how current assumptions in practice related to the embedment strength in relation to the fibre orientation should be reconsidered.

CLT structures are commonly used nowadays. Due to their configuration with cross layers, it is commonly assumed that brittle failure modes in the connections are prevented. However, as shown in this work, it is not always the case. Further works are required to improve the understanding of the underlying mechanisms and improve their assessment.

CRediT authorship contribution statement

Boris Azinović: Conceptualization, Investigation, Writing – original draft, Writing – review & editing, Resources. **José Manuel Cabrero:** Conceptualization, Methodology, Formal analysis, Writing – original draft, Writing – review & editing. **Henrik Danielsson:** Conceptualization, Methodology, Writing – original draft, Writing – review & editing, Validation. **Tomaž Pazlar:** Investigation, Writing – original draft, Writing – review & editing, Resources.

Declaration of Competing Interest

The authors declare that they have no known competing financial interests or personal relationships that could have appeared to influence the work reported in this paper.

Acknowledgements

The current research has received support within ERA-NET Cofund ForestValue by MIZŠ, VINNOVA, FORMAS, STEM, BMLFUW, FNR and MINECO-AEI and has received funding from the European Union's Horizon 2020 research and innovation programme under grant agreement N° 773324. The financial support provided by Fachagentur Nachwachsende Rohstoffe e.V. (FNR) of the German Federal Ministry of Food and Agriculture (BMEL) and the Spanish Ministerio de Ciencia, Innovación y Universidades – Agencia Estatal de Investigación under contract PCI2019-103591 AEI is gratefully acknowledged.

References

[1] Mohammad M, Blass H, Salenikovich A, Ringhofer A, Line P, Rammer D, et al. Design approaches for CLT connections. Wood Fiber Sci 2018;50(Special):27–47.
[2] Uibel T, Blaß HJ. Joints with dowel type fasteners in CLT structures, in: Focus Solid Timber Solut.-Eur. Conf. Cross Laminated Timber CLT Bath, 2013: pp. 119–136.
[3] Jorissen A, Fragiacomo M. General notes on ductility in timber structures. Eng Struct 2011;33(11):2987–97.
[4] Fragiacomo M, Dujic B, Sustersic I. Elastic and ductile design of multi-storey crosslam massive wooden buildings under seismic actions. Eng Struct 2011;33(11):3043–53.
[5] Hansson EF. Analysis of structural failures in timber structures: Typical causes for failure and failure modes. Eng Struct 2011;33:2978–82.
[6] Sandhaas C, Munch-Andersen J, Dietsch P, Jockwer R. Design of Connections in Timber Structures. GmbH: Shak.-Verl; 2018.
[7] Cabrero JM, Stepinac M, Ranasinghe K, Kleiber M. Results from a questionnaire for practitioners about the connections chapter of Eurocode 5. In: Dietsch P, Sandhaas C, Munch-Andersen J, editors, Des. Connect. Timber Struct. State—Art Rep. COST Action FP1402WG3, 2018: p. 3.
[8] Yurrita M, Cabrero JM, Moreno-Zapata E. Brittle failure in the parallel-to-grain direction of timber connections with small diameter dowel-type fasteners: A new design model for plug shear. Eng Struct 2021;241:112450. https://doi.org/10.1016/j.engstruct.2021.112450.
[9] Yurrita M, Cabrero JM. New design model for brittle failure in the parallel-to-grain direction of timber connections with large diameter fasteners. Eng Struct 2020;217:110557. https://doi.org/10.1016/j.engstruct.2020.110557.
[10] Cabrero JM, Yurrita M. Performance assessment of existing models to predict brittle failure modes of steel-to-timber connections loaded parallel-to-grain with dowel-type fasteners. Eng Struct 2018;171:895–910. https://doi.org/10.1016/j.engstruct.2018.03.037.
[11] Cabrero JM, Yurrita M. A review of the existing models for brittle failure in connections loaded parallel to the grain. In: Dietsch P, Sandhaas C, Munch-Andersen J, editors. Des. Connect. Timber Struct. State–-Art Rep. COST Action FP1402WG3. Aachen: Shaker Verlag; 2018. p. 127–41.
[12] Zarnani P, Quenneville P. New design approach for controlling brittle failure modes of small-dowel-type connections in Cross-laminated Timber (CLT). Constr Build Mater 2015;100:172–82. https://doi.org/10.1016/j.conbuildmat.2015.09.049.
[13] EN 1995-1-1:2004+A2:2014 - Eurocode 5: Design of timber structures - Part 1-1: General - Common rules and rules for buildings, Eurocode 5. (2014).
[14] I. ASTM, ASTM D5457-21a Standard Specification for Computing Reference Resistance of Wood-Based Materials and Structural Connections for Load and Resistance Factor Design, ASTM, 2021.
[15] Association CS. CSA O86-09 Engineering design in wood, Canada; 2019.
[16] Schenk M, Gonzalez-Serna P, Cabrero JM. Future research on cross laminated timber (CLT) for multi-storey buildings - A questionnaire among engineers active in practice, in: Santiago (Chile); 2021.
[17] Wallner-Novak M, Koppelhuber J, Pock K. Cross-Laminated Timber Structural Design, proHolz Austria; 2014.
[18] Borgström E, Fröbel J, editors, The CLT Handbook, 1st ed., Swedish Wood, Stokholm; 2019.
[19] Bogensperger T, Moosbrugger T, Schickhofer G, editors, BSPhandbuch, Holz-Massivbauweise in Brettsperrholz, Verlag der Technischen Universität Graz; 2010.
[20] DIBt. ETA 11-0284 Screws for use in timber construction; 2019.
[21] OIB. ETA 14-0349 Solid wood slab element to be used as a structural element in buildings; 2020.
[22] OIB. ETA 12-0347 Solid wood slab element to be used as a structural element in buildings; 2020.
[23] Jorissen AJM. Double shear timber connections with dowel type fasteners. The Netherlands: Delft University Press Delft; 1998.
[24] S. New Zealand, NZS 3603:1993 Timber Structures Standard, NZS; 1993.
[25] Quenneville P. New Zealand specific amendments to AS 1 720.1–2010 (Normative); 2017.
[26] Zarnani P, Quenneville P. Wood block tear-out resistance and failure modes of timber rivet connections: A stiffness-based approach. J Struct Eng 2014;140:04013055. https://doi.org/10.1061/(ASCE)ST.1943-541X.0000840.
[27] ISO 6891:1983 Timber structures — Joints made with mechanical fasteners — General principles for the determination of strength and deformation characteristics, (n.d.).
[28] EN 12512:2005, Timber structures - Test methods - Cyclic testing of joints made with mechanical fastener, CEN; 2005.
[29] Yurrita M, Cabrero JM, Quenneville P. Brittle failure in the parallel-to-grain direction of multiple shear softwood timber connections with slotted-in steel plates and dowel-type fasteners. Constr Build Mater 2019;216:296–313. https://doi.org/10.1016/j.conbuildmat.2019.04.100.
[30] EN 14358:2016, Timber Structures - Calculation and verification of characteristic values, CEN; 2016.
[31] EN 338. Structural timber - Strength classes, CEN; 2016.
[32] Steyerberg EW, Vickers AJ, Cook NR, Gerds T, Gonen M, Obuchowski N, et al. Assessing the performance of prediction models. Epidemiology 2010;21:128–38. https://doi.org/10.1097/EDE.0b013e3181c30fb2.
[33] Chirico N, Gramatica P. Real external predictivity of QSAR models: How to evaluate It? Comparison of different validation criteria and proposal of using the concordance correlation coefficient. J Chem Inf Model 2011;51:2320–35. https://doi.org/10.1021/ci200211n.
[34] Chirico N, Gramatica P. Real external predictivity of QSAR models. Part 2. New intercomparable thresholds for different validation criteria and the need for scatter plot inspection. J Chem Inf Model 2012;52(8):2044–58.
[35] Gramatica P, Sangion A. A historical excursus on the statistical validation parameters for QSAR models: a clarification concerning metrics and terminology. J Chem Inf Model 2016;56:1127–31. https://doi.org/10.1021/acs.jcim.6b00088.
[36] Golbraikh A, Tropsha A. Beware of q^2! J Mol Graph Model 2002;20:269–76. https://doi.org/10.1016/S1093-3263(01)00123-1.
[37] Alexander DLJ, Tropsha A, Winkler DA. Beware of R^2: simple, unambiguous assessment of the prediction accuracy of QSAR and QSPR models. J Chem Inf Model 2015;55:1316–22. https://doi.org/10.1021/acs.jcim.5b00206.